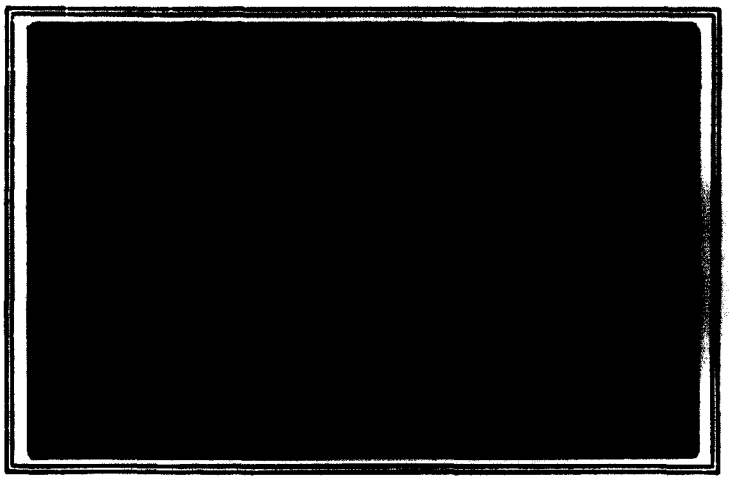

UPPSALA UNIVERSITY

INSTITUTE OF PHYSICS

HYPERFINE STRUCTURE, NUCLEAR SPINS AND MAGNETIC MOMENTS OF SOME CESIUM ISOTOPES

C. Ekström, S. Ingelman, G. Wannberg
and M. Skarestad

UUIP-953 March 1977

SW ISSN 0042-0263

HYPERFINE STRUCTURE, NUCLEAR SPINS AND MAGNETIC MOMENTS OF SOME CESIUM ISOTOPES

C. Ekström *)
Department of Physics, Chalmers University of Technology and University of Gothenburg, Gothenburg, Sweden.

S. Ingelman and G. Wannberg
Institute of Physics, University of Uppsala, Uppsala, Sweden.

M. Skarestad +)
E.P. Division, CERN, Geneva, Switzerland.

and

The ISOLDE Collaboration, CERN, Geneva, Switzerland.

ABSTRACT

Using an atomic-beam magnetic resonance apparatus connected on-line with the ISOLDE isotope separator, CERN, hyperfine structure measurements have been performed in the $^2S_{\frac{1}{2}}$ electronic ground state of some cesium isotopes. An on-line oven system which efficiently converts a mass separated ion-beam of alkali isotopes to an atomic-beam is described in some detail. Experimentally determined nuclear spins of ^{120,121,121m,122,122m,123,124,126,128,130m,135m}Cs and magnetic moments of ^{122,123,124,126,128,130}Cs are reported and discussed in terms of different nuclear models. The experimental data indicate deformed nuclear shapes of the lightest cesium isotopes.

---

*) Present address : EP Division, CERN, CH-1211 Geneva 23, Switzerland.

+) On leave from Department of Chemistry, University of Oslo, N-1000 Oslo 3, Norway.

1. INTRODUCTION

The importance of systematic investigations of nuclear spins and moments as a test of different models for nuclear structure is well recognized. The experimental situation, however, becomes increasingly complicated as one moves away from the line of beta-stability, because of shorter half-lives, lower production yields and of the large number of reaction products. These complications are to a large extent overcome in on-line experiments using an intermediate isotope separation step. The atomic-beam magnetic resonance (ABMR) apparatus connected on-line with the ISOLDE isotope separator at CERN has proven to be a useful tool in hyperfine structure investigations of short-lived nuclides far from beta-stability. We here report briefly on the on-line operation of the system, and on the measurements of nuclear spins and magnetic moments of some cesium isotopes. In an earlier paper [1] we described the atomic-beam experiments at ISOLDE on some moderately short-lived gold isotopes using off-line techniques.

2. EXPERIMENT

2.1 General procedure

A simplified drawing of the atomic-beam apparatus is shown in fig. 1. In the on-line experiments, the ion-beam from the isotope separator (1) is deflected 90^0 by the electrostatic deflector plates (3) and focused by the electrostatic quadrupole doublet (7) to a small spot at the oven position of the atomic-beam apparatus, from where it is continuously evaporated in the form of free atoms. The sixpole magnet (9) acts as a state selector on the atomic-beam; atoms with positive m_J-values are focused into the central region (10), while atoms with negative m_J-values are defocused (cf. the lower part of fig. 1 showing the narrow beam space with a heavily enlarged radial scale). By inducing transitions from a state with positive m_J-value to one

with negative m_J-value with the external r.f.-field, the atoms are defocused by the fourpole analysing magnet (11) and reach the collector (12). Otherwise, the atoms are focused and hit the cooled central obstable in the analysing magnet, where they are adsorbed. The activity passing through the apparatus is collected on discs fed from a supply (13) and counted in an on-line detector system (14). A mini-computer handles the data acquisition and controls most of the experimental routines, such as changing the r.f. frequencies and transporting the collector discs within the collector-detector system. A technical description of the atomic-beam apparatus will be published in a forthcoming paper [2]. We therefore restrict ourselves to details pertinent to the experiments on the cesium isotopes.

2.2 Beam production

The isotopes studied in this work were produced by spallation reactions in a liquid lanthanum target bombarded with 600 MeV protons from the CERN synchro-cyclotron. Among the volatile reaction products, cesium is selectively ionized by surface ionization and subsequently mass separated in the ISOLDE on-line isotope separator [3,4]. The experimental yields of cesium isotopes from a molten lanthanum target as measured at the collector side of the separator are given in fig. 2. The peak yield of 7 nA represents an improvement of a factor 500 as compared to the data before the reconstruction of the synchro-cyclotron and the ISOLDE facility. This improvement is of course of vital importance for the atomic-beam experiments, requiring typically 10^6-10^7 atoms/sec.

The atomic-beam oven is in the case of on-line operation simply a metal foil heated by resistance heating. It is mounted at a 45^0 angle to the incoming ion-beam as well as to the optical axis of the atomic-beam apparatus. This arrangement is

described in ref.[2] . The experiments on the alkali elements, however, require particular attention as to the choice of oven-foil material. The following conditions should be fulfilled :

i) low work function,
ii) thermochemically stable at temperatures above 1000° C,
iii) low sensitivity to induced heterogenity,
iv) easy to manufacture.

The first requirement appears because of the necessity to convert the incoming ion-beam to an atomic-beam at the foil. According to the Saha-Langmuir formula, the ionization efficiency of a surface is given by :

$$\eta = \frac{f^+}{f_p} = \{1 + C \exp(W - \phi)/kT\}^{-1}, \qquad (1)$$

where f^+ = flux of ions leaving the surface, f_p = flux of incoming ions, C = statistical constant, W = first ionization potential of the atom, ϕ = electron work function of the surface, k = Boltzmanns constant and T = the absolute temperature. For the alkali elements, the constant C takes the value 2. The neutralization efficiency is then :

$$\xi = 1 - \eta. \qquad (2)$$

The neutralization efficiencies as functions of the work function are shown in fig. 3 for the alkali elements potassium, rubidium and cesium having ionization potential W = 4.34, 4.18 and 3.89 eV [5], respectively. An oven foil temperature of 1000° C is assumed. Foils of different refractory metals such as Nb, Mo, Ta, W, Re and Pt, having work functions $\phi > 4$ eV, have been tested and found to give a low atom to ion ratio of cesium in accordance with the expectations. We have found that an oven foil of tantalum covered by a thin layer of yttrium satisfactorily meets the requirements above :

i) Polycrystalline yttrium metal has a work function $\phi \approx 3.2$ eV [6]. This value, however, has been measured under pure conditions (clean surface, high vacuum). In our oven section, where the pressure is in the range 10^{-6} - 10^{-5}torr, this condition is probably not fulfilled. Heterogenity induced by O_2 or N_2 is likely to exist, but it is difficult to predict to which extent it will influence the work function of the surface [7]. In any case, it is promising to note that also the oxide of yttrium has a low work function, $\phi \sim 3.1$ eV [6].

ii) The melting point of yttrium is 1509° C [5]. From vapour pressure data [8] it can be calculated that the evaporation loss of yttrium corresponds to $\approx$ 1 mg/cm^2 · hour at 1200° C increasing to $\approx$ 25 mg/cm^2 · hour at 1400° C. This means that the Y/Ta foil can be operated at temperatures up to 1400° C.

iii) Yttrium is a stable metal which can be stored at room temperature in air. The corrosion rate is about 1 mg/cm^2 · day only [9].

iv) The foil is easily prepared by melting some 20 mg yttrium on a 50 μm Ta-backing in vacuum.This amount corresponds to about 100 mg/cm^2. The Ta-backing, which does not alloy with yttrium, gives the foil the necessary mechanical stability at high temperatures.

In order to understand the release mechanism of alkali atoms from an Y-Ta foil, and to determine the evaporation temperatures needed, a separate study was made on implanted isotopes of ^{84}Rb ($T_{\frac{1}{2}}$ = 33 d). The amount of ^{84}Rb was measured before the experiment with a NaI-detector. The sample was then placed in a high vacuum unit and heated to a certain temperature for a certain period of time. After the heating period, the sample activity was measured again. This cycle was repeated 3 times at 3 different temperatures. The results, given in fig. 4, will be discussed below.

The incoming 60 keV alkali ions penetrate the surface at a maximum range of typically some 0.05 μm [10]. The initial ion trapping is followed by release processes which are thermally activated. Two separate processes are of importance, i.e. bulk diffusion of the product to the surface and evaporation of the product from the surface. The relative importance of the processes depends on the activation energies in the two cases. The surface desorption step is commonly described by the equation :

$$\tau = \tau^0 \, e^{Q/RT} \qquad (3)$$

where τ^0 is the time of oscillation of the absorbed atom perpendicular to the surface, Q is the desorption energy, R the gas constant and T the absolute temperature. For the alkali elements τ^0 and Q have been measured to be $\approx 10^{-13}$s and ≈54 kcal/mol, respectively [11]. This means that for rubidium, the lingering time τ at 800° C takes the value $\approx 8 \cdot 10^{-3}$s and at 1200°C $\approx 8 \cdot 10^{-6}$s. These values are far below the time constants found in fig. 4, indicating that the bulk diffusion step is the time consuming release mechanism. Also, the non-exponential form of the release curves support this explanation (ref. [3] p. 123).

The half-lives of alkali nuclides available for atomic-beam measurements are generally above 20 s. The nuclides with shorter half-lives found on the extreme wings of the yield curves are generally produced in too low yield to allow atomic-beam experiments. This means that a foil temperature of about 1000° C should be sufficient to ensure no significant decay loss on the foil. However, in a few cases extremely short-lived nuclides may be produced in high yield, like e.g. ^{219}Fr ($T_{\frac{1}{2}}$ = 20 ms) from a high temperature uranium carbide target. In order to judge the prospects of such rare but interesting cases, we have made a rough extrapolation of the delay (in terms of the time for 50% release) as a function of temperature. It is seen in fig. 5 that half-lives

below the 100 ms level can be handled by pushing the temperature to the limit of 1400° C.

The on-line oven system described above has shown to be very efficient when studying short-lived activities. It has been used in this investigation of cesium isotopes, except in the experiments on ^{135m}Cs (53 min) where the conventional off-line oven proved to be superior. In the latter experiments, the sources were collected on aluminium foils in the off-line collector position (2) in fig. 1.

2.3 Detection

The activity passing through the atomic-beam apparatus was collected on aluminium foils and subsequently measured. Thin (1 mm) plastic scintillators, mounted on PM-tubes, were used for the detection of the β^+-decaying isotopes, i.e. the main part of the isotopes studied. The isomer ^{135m}Cs, decaying by two γ-transitions (841 and 786 keV) to the ground state, was measured with Ge(Li) and NaI detectors.

The signal to background ratio obtained in the experiments using the on-line oven system was of the order 20:1 in a typical spin measurement. It reduced to about 5:1 in the high field measurements where a smaller number of hyperfine states contributes to the signal.

2.4 Measurements and results

The experiments were performed in the 6s $^2S_{\frac{1}{2}}$ electronic ground state of cesium having the splitting factor $g_J = 2.0025410(24)$ [12]. The hyperfine levels of a $J = \frac{1}{2}$ atom are given in the (F, m_F)- representation by the Breit-Rabi formula

$$W(F,m_F) = -\frac{h\Delta\nu}{2(2I+1)} - g'_I \mu_B B m_F \pm \frac{h\Delta\nu}{2}\sqrt{1 + \frac{4m_F}{2I+1}x + x^2} \quad (4)$$

where $x = (g_I' + g_J)(\mu_B B/h)(1/\Delta\nu)$. The positive sign refers to the hyperfine level $F = I + \frac{1}{2}$ and the negative sign to the level $F = I - \frac{1}{2}$. The hyperfine structure separation $\Delta\nu$ is related to the dipole hyperfine constant a by :

$$\Delta\nu = a(I + \tfrac{1}{2}). \qquad (5)$$

The energy level diagram for an $I = 1$ atom is shown in fig. 6, assuming a positive value of a.

In weak external magnetic fields B, the resonance frequency ν for allowed transitions between substates belonging to the same hyperfine level is given by the expression :

$$\nu = g_J \frac{\mu_B B}{h} \frac{1}{2I+1} \qquad (6)$$

neglecting the small term in g_I'. In the case $I = 1$, the single-quantum transition $(F = {}^3/_2, m_F = -\frac{1}{2}) \rightarrow (F = {}^3/_2, m_F = -{}^3/_2)$ is indicated in fig. 6 by an arrow. Normally this transition requires moderate r.f. power to be saturated. By increasing the r.f. power, the double-quantum $({}^3/_2, {}^1/_2) \rightarrow ({}^3/_2, -{}^3/_2)$ and triple-quantum $({}^3/_2, {}^3/_2) \rightarrow ({}^3/_2, -{}^3/_2)$ transitions may also be induced. In the weak-field region, these multiple-quantum transitions appear at the same frequency as that of the single-quantum transition. It is thus of importance to apply sufficient r.f. power in order to get strong resonance signals, particularly in the case of high spin values where the hyperfine levels are split into a large number of magnetic sub-states.

The spin measurements in cesium were made at 2 or 3 different settings of the external magnetic field in the range 80 - 290 μT. The results obtained are given in table 1. One may note the previously unknown isomer in ^{121}Cs, observed in the spin-separated samples. The $I = {}^3/_2$ and $I = {}^9/_2$ states showed to

have similar half-lives, $T_{\frac{1}{2}} \approx 2$ min, and to be produced in about equal amounts. It was, however, not possible to determine whether the $^3/_2$ or $^9/_2$ state corresponds to the ground state. A careful search was made without success for the high spin isomer in ^{120}Cs reported by Genevey-Rivier et al [13].

By increasing the external magnetic field and observing the deviations from the linear Zeeman-effect, it is possible to determine the hyperfine structure separation $\Delta\nu$ and the dipole hyperfine constant a. These measurements were performed in the doubly odd nuclides ^{122,124,126,128,130}Cs, all having a nuclear ground state spin I = 1, and in the I = ½ odd-A nucleus ^{123}Cs. The single- and double-quantum transitions were identified in an external magnetic field of 2.25 mT and the single-quantum transitions were subsequently followed up to 23.2mT. The resonance curves obtained for the isotopes ^{122}Cs (21 sec) and ^{130}Cs (30 min) at 15.0 mT are given in fig. 7a and 7b, respectively. The curves show the same line shape as the potassium calibration line at this field, a slight broadening towards lower frequencies, and line widths FWHM of about 80 kHz.

In order to increase the accuracy of the hfs separation in ^{122}Cs, we decided to try a measurement in weak external field of the $\Delta F = 1$ transitions $(^3/_2, -^1/_2) \leftrightarrow (^1/_2, ^1/_2)$, $(^3/_2, ^1/_2) \leftrightarrow (^1/_2, -^1/_2)$ and $(^3/_2, ^3/_2) \leftrightarrow (^1/_2, ^1/_2)$; the frequencies of the first two transitions being degenerate and field independent to second order. This resonance line is thus expected to be narrow, FWHM of the order 10 kHz, with the r.f. geometry used. The r.f. generator to be used in such an experiment therefore should have good resolution (5 kHz or better), as well as good longtime stability and a useful output power level to overcome inevitable matching losses. Preferably, it should also be programmable in order to retain the automated measuring facilities. A system operating in the region around 620 MHz and satisfying the requirements outlined above was constructed. The solution, illustrated schematically in fig. 8, was shown to

perform satisfactorily on all accounts. The results from the frequency scan in a field of about 30 μT is shown in fig. 9.

In table 2 are collected the results from the hfs measurements in the cesium isotopes. The uncertainty of the calibration and resonance frequencies is taken to be a quarter of the line widths. In case of field drifts during the experiment, the error has been increased correspondingly. The residual, χ^2 and the hfs constants obtained in a least-squares fit of the experimentally observed resonances to the Breit-Rabi formula, eq. 4, assuming either a positive or a negative sign of the nuclear g-factors, are also given in table 2.

Performing a confidence test of the sign assignments to the g-factors, the assumption of a positive moment in the isotopes ^{123,124,126,128,130}Cs proved to be valid at a high level of confidence. In ^{122}Cs, however, the magnitude of the magnetic moment showed to be too small to have a decisive influence (a positive sign is slightly preferred) upon the godness of the fit for either choice of sign. The resulting hfs separations and dipole hyperfine constants are given in table 3. The errors quoted are one standard deviation. The present data on the isotope ^{130}Cs represent an improvement of a factor 30 in accuracy compared to the results obtained by Nierenberg et al. [14]. From their data, the sign of the moment could not be determined.

The magnetic moments of the cesium isotopes are easily calculated from the dipole constants by a direct comparison with the known values in the stable isotope ^{133}Cs.

$$\mu_I = \mu_{I133} \frac{a\, I}{a_{133} I_{133}} (1 + A_\Delta^{133}) \qquad (7)$$

where μ_{I133} = 2.582065(9) n.m. (diam. corr.) [15],
a_{133} = 2298.157943 MHz [16],
I_{133} = $^7/_2$ [15].

A large uncertainty is, however, introduced by the unknown hyperfine anomaly $^{A}\Delta^{133}$. We give in table 3 the magnetic moments calculated under the assumption of $^{A}\Delta^{133} = \pm 1\%$. The hyperfine anomaly may, however, in certain cases exceed this value; and in the isotope ^{122}Cs, having a very small magnetic moment, it probably would be more appropriate to give an absolute error (cf. section 3 in ref. [17]).

The variation of the magnetic moments of the isotopes $^{120-130}$Cs with mass number is shown in fig. 9. Note the rapid increase in magnitude for the doubly-odd isotopes with increasing mass number, and the relatively constant values for the odd-A isotopes.

3. DISCUSSION

3.1 General considerations

A general idea about the nuclear properties to be expected in the region around the neutron-deficient cesium isotopes may be obtained by inspecting the partial nuclear chart shown in fig. 11. In the region enclosed by 50 = (N, Z) = 82, the stable and identified radioactive nuclides are found in the corner $Z > 50$ and $N < 82$. Close to these shell closures, the spherical shell model [18] is expected to give a good description of the nuclear properties. At the centre of the region enclosed by 50 = (N, Z) = 82, strongly deformed nuclear shapes have been suggested to appear [19,20]. The iso-deformation curves for prolate shapes, as calculated by Arseniev [21] are incorporated in fig. 11. Between these regions of extreme nuclear shapes, we have a transition region. Here, we may expect a competition between vibrational and rotational structures, and even within the same nucleus one may observe states of both spherical and deformed shapes, the latter often of triaxial character [22,23]. Two distinct types of band structure may be observed in a nucleus with moderate deformation, if the Fermi surface is located close either

to the lower or upper part of levels originating from a high-spin shell model state [24]. In a prolate nucleus, decoupled bands appear for particle states and rotational bands for hole states. The levels originating from low-spin shell model states are in the transition region often strongly mixed, making the interpretations of nuclear spins, moments and level structure very complicated.

3.2 Discussion of nuclear spins and moments in the Cesium region

The shell model states $g_{7/2}$, $d_{5/2}$, $h_{11/2}$, $s_{1/2}$ and $d_{3/2}$ are available as odd-proton as well as odd-neutron states in the region $50 \leq (N, Z) \leq 82$. For obvious reasons, the main part of odd-proton ground states are characterized either by $g_{7/2}$ or $d_{5/2}$. Similarly, in odd-neutron nuclei we find, close to N = 82, mainly $s_{1/2}$ or $d_{3/2}$ ground states. The low-lying level structure of nuclei with $N \geq 77$ has been discussed previously in connection with our spin-measurements in isotopes of the elements promethium-gadolinium [25]. To this may be added the spin $I = {}^{19}/_{2}$ of ^{135m}Cs which may be interpreted as a three-quasiparticle state, in which the $h_{11/2}$ neutron state has to be involved.

A large part of the nuclei in the region $50 \leq (N, Z) \leq 82$ which are experimentally accessible may be regarded as transitional. The first experimental results on band structure associated with the rotation-aligned coupling scheme [24] were obtained in this region in a number of lanthanum isotopes [26]. Since the Fermi surface in lanthanum is located at the lower part of the levels originating from the $h_{11/2}$ shell model state, the observed decoupled bands based on the ${}^{11}/_{2}^{-}$ isomeric states clearly indicate prolate-type deformation. Similar decoupled bands have later been observed in isotopes of cesium, praseodymium and promethium [27-30]. In odd-A isotopes of antimony and iodine, rotational bands built on the ${}^{9}/_{2}^{+}$ isomeric states have been identified [31,32]. This fact again points at prolate-type

shapes, since here the Fermi surface is situated above the levels originating from the $g_{9/2}$ shell model state. The Fermi surface in odd-neutron nuclei close to N = 82 is located at the upper part of the levels from the $h_{11/2}$ shell. Rotational-like bands have here been observed in a large number of nuclei indicating prolate-type shapes [33-37]. The same conclusion may be drawn from the decoupled bands identified in the light barium isotopes with N = 65 and N = 67, occupying the low-spin levels from the $h_{11/2}$ shell [38].

Recent theoretical calculations incorporating asymmetric nuclear shapes reproduce satisfactorily the band structures of high-spin unique-parity states in the transition region [22,23]. These results are consistent with those obtained from an investigation [39] of level schemes and transition probabilities in doubly-even nuclei, revealing spherical shapes near the shell closures at Z = 50 and N = 82, asymmetric shapes ($20^0 < \gamma < 30^0$) and moderate values of the deformation parameter β in a transition region, and, further away from the shell closures, a transition to more symmetric shapes and to stronger β-deformations.

The results above do not, however, necessarily apply to the low-spin states in the transitional and deformed regions. Theoretical potential energy surfaces generally show two minima close in energy, one at prolate and the other at oblate deformation, the barrier in the γ-direction being very low.

Since it seems possible to get a consistent picture of the low-spin states at the centre of the region $50 \leq (N, Z) \leq 82$ by assuming a prolate deformation, we will attempt an interpretation of the light cesium isotopes in terms of the strong-coupling model, keeping in mind that many of the properties are as well reproduced by the intermediate coupling version of the unified model [40,41].

Single-particle energy levels as functions of the quadrupole deformation ε have been calculated within the Nilsson model, employing several sets of shell parameters, e.g. the parameters valid in the strongly deformed rare-earth region, the parameters obtained by an extrapolation from the actinides and the rare-earths to the centre of the region $50 \leq (N, Z) \leq 82$, and the "modified" parameters suggested by Ragnarsson and Nilsson [42]. The Nilsson diagrams obtained using the "extrapolated" shell parameters $\kappa_p = 0.0662$, $\mu_p = 0.540$ and $\kappa_n = 0.0637$, $\mu_n = 0.450$ are shown in fig. 12. In the "rare-earth" diagram for odd protons, the energy difference between the levels $g_{7/2}$ and $d_{5/2}$ is larger and the orbitals $[420\ ^1/_2]$ and $[422\ ^3/_2]$ do not intersect for ε-values smaller than 0.3. For the odd neutrons, the $h_{11/2}$ state is located between the states $s_{1/2}$ and $d_{3/2}$. Using the "modified" parameters, we find that the level order between the proton levels $g_{7/2}$ and $d_{5/2}$ is reversed, and that the $h_{11/2}$ neutron state is located above the $s_{1/2}$ and $d_{3/2}$ states. The "extrapolated" diagrams shown in fig. 12 thus represent medium cases to the "rare-earth" and "modified" diagrams.

The nuclear ground state spins of the odd-A cesium isotopes ^{123,125,127,129}Cs have been measured with the result $I = {}^1/_2$ in all cases. Positive parity is suggested by spectroscopic works. These results are accounted for by the Nilsson orbital $[420\ ^1/_2]$ which, in the level diagram shown in fig. 12 is occupied by the 55th proton of cesium in a wide range of positive deformation values. The experimental magnetic moments of these isotopes are well reproduced by the theoretical moment of the level $[420\ ^1/_2]$, assuming $g_s = 0.6\ g_s^{free}$, $g_l = 1$, $g_R = 0.45$ and the shell parameters from the rare-earth region. The moments obtained using the extrapolated parameters are slightly too small, $\Delta\mu \approx 0.2$ n.m., while the "modified" values are considerably smaller, $\Delta\mu \approx 0.5 - 1.0$ n.m.

In a recent spectroscopic work on the decay of ^{127}Ba, Beyer et al [43] propose the strongly fed $^{3}/_{2}^{+}$ excited state in ^{127}Cs to be a rotational member of the ground state band. Furthermore, the low-lying states with $I^{\pi} = {}^{5}/_{2}^{+}$, ${}^{3}/_{2}^{+}$, ${}^{7}/_{2}^{+}$ and ${}^{11}/_{2}^{-}$ are shown to have the same sign of the deformation. These states may consequently be given the assignments [413 $^{5}/_{2}$], [411 $^{3}/_{2}$] or [422 $^{3}/_{2}$], [404 $^{7}/_{2}$] and $^{11}/_{2}^{-}$[550 $^{1}/_{2}$], respectively. A similar interpretation of the low-lying states in ^{137}Pr has recently been attempted by Klewe-Nebenius et al [29]. We may also mention our earlier spin measurements in the odd-Z elements lanthanum and praseodymium [44,45]. The $^{3}/_{2}^{+}$ ground states in ^{131}La and ^{135}Pr may be assigned [411 $^{3}/_{2}$], and the $^{5}/_{2}^{+}$ ground state in ^{133}Pr [413 $^{5}/_{2}$].

In the isotope ^{121}Cs we observe two isomers of similar half-lives having the nuclear spins $I = {}^{3}/_{2}$ and $I = {}^{9}/_{2}$. Assuming a nuclear deformation $\varepsilon \sim 0.25$, the spin values may be interpreted as arising from the orbitals [422 $^{3}/_{2}$] and [404 $^{9}/_{2}$], the latter one originating from the $g_{9/2}$ shell and raising steeply with increasing deformation. Further evidence for deformed nuclear shapes in the light cesium isotopes is given by the nuclear ground state spin of ^{119}Cs, $I = {}^{9}/_{2}$, measured by the optical pumping group at ISOLDE [46].

The doubly-odd cesium isotopes in the mass range A = 122-130, all have a nuclear ground state spin and parity $I^{\pi} = 1^{+}$. The magnetic moments, on the other hand, show a drastic variation in magnitude (cf. fig. 10). The large difference between the magnetic moments of ^{122}Cs and ^{124}Cs may be explained by assuming the proton orbitals [422 $^{3}/_{2}$] and [420 $^{1}/_{2}$], respectively, coupled to a [411 $^{1}/_{2}$] neutron. This interpretation is consistent with the assumption that the neighbouring nuclei ^{121}Cs and ^{123}Cs are characterized by [422 $^{3}/_{2}$] and [420 $^{1}/_{2}$], respectively. The further increase in magnitude for the heavier cesium isotopes

is, however, not accounted for by the predictions of the Nilsson model. It seems that these nuclei have to be treated as transitional, with an increasing influence of the $1^+(p\ d_{5/2}\ n\ d_{3/2})$ shell model configuration, having a nuclear magnetic moment of about 2 n.m.

The neutron orbital $[514\ ^9/_2]$ probably contributes to the nuclear spin I = 5 of the isomeric state in ^{130}Cs. We have earlier measured [44,45] the nuclear spins in the N = 75 isotones ^{133}Ce and ^{135}Nd with the result I = $^9/_2$, and proposed the assignment $[514\ ^9/_2]$. The $^9/_2^-$ states in ^{131}Ba, ^{133}Ce and ^{135}Nd form the band heads of the rotation levels discussed above.

Returning again to the light cesium isotopes, the high-spin I = 8 isomer in ^{122}Cs may be explained by coupling the proton orbital $[404\ ^9/_2]$, appearing in ^{121}Cs, with the neutron orbital $[523\ ^7/_2]$. This configuration implies a negative parity of the state.

The doubly-odd isotope ^{120}Cs with a nuclear spin I = 2 may be given the same nuclear configuration as ^{122}Cs, namely $p[422\ ^3/_2]$ $n[411\ ^1/_2]$, this time, however, coupled according to the rules of Gallagher and Moszkowski [47].

ACKNOWLEDGEMENTS

The authors would like to express their gratitude to Prof. I. Lindgren for continuous support of the project, to the members of the ISOLDE Collaboration for helpful assistance and discussions, and to Dr. H. Rubinsztein and Mr. B. Hellsing for assistance in part of the measurements. Thanks are also due to Mr. K. Ängvard of Hewlett-Packard Sweden AB for help during the alignment of the 620 MHz source.
This work is supported financially by the Swedish Council for Atomic Research.

REFERENCES

[1] C. Ekström, I. Lindgren, S, Ingelman, M. Olsmats and G. Wannberg, Phys. Lett. 60B, 146 (1976).

[2] C. Ekström, S. Ingelman and G. Wannberg, to be published.

[3] The ISOLDE Isotope Separator On-Line Facility at CERN, eds. A. Kjelberg and G. Rudstam, CERN Report 70-3, 1970.

[4] H.L. Ravn, L.C. Carraz, J. Denimal, E. Kugler, M. Skarestad, S. Sundell and L. Westgaard, Nucl. Instr. 139, 267 (1976).

[5] Handbook of Chemistry and Physics, 55th Ed. (The Chemical Rubber Co., Cleveland, Ohio, 1975) p. E67.

[6] Atomic Sources and Detectors, eds. W.J. Vernon and L.S. Howard (Academic Press, New York, 1967) p. 21.

[7] M. Karminsky in Atomic and Ionic Impact Phenomena on Metal Surfaces (Springer-Verlag, Berlin, 1965) p. 8.

[8] Selected Values of the Thermodynamic Properties of the Elements, eds. R. Hultgren, P.D. Desai, D.T. Hawkins, M. Gleiser, K.K. Kelly and D.D. Wagman (American Society for Metals, Ohio, 1973) p. 559.

[9] The Rare-Earths, eds. F.H. Spedding and A.H. Daane (R.E. Krieger Publishing Co. Inc., New York, 1971) p. 166.

[10] F. Brown, G.C. Ball, D.A. Channing, L.M. Howe, J.P.S. Pringle and J.L. Whitton, Nucl. Instr. 38, 249 (1965).

[11] Absorption and Desorption Phenomena, ed. F. Ricca (Academic Press, New York, 1972) p. 169.

[12] K.D. Böklen, W. Dankwort, E. Pitz and S. Penselin, Z. Physik 200, 467 (1967).

[13] J. Genevey-Rivier, A. Charvet, G. Marguier, C. Richard-Serre, J. D'Auria, A. Huck, G. Klotz, A. Knipper and G. Walter, submitted to Nucl. Phys.

[14] W.A. Nierenberg, H.A. Shugart, J.B. Silsbee and R.J. Sunderland, Phys. Rev. 112, 186 (1958).

[15] V.S. Shirley and C.M. Lederer, Table of Nuclear Moments, Hyperfine Interactions Studied in Nuclear Reactions and Decay (Vol. II), invited papers, eds. E. Karlsson and R. Wäppling (Almqvist and Wiksell International, Stockholm-New York, 1975).

[16] Definition, time system AT1.

[17] C. Ekström, G. Wannberg and Y.S. Shishodia, Hyperfine Interactions 1, 437 (1976).

[18] A. de-Shalit and I, Talmi, Nuclear Shell Theory (Academic Press, New York, 1963).

[19] R.K. Sheline, T. Sikkeland and R.M. Chanada, Phys. Rev. Lett. 7, 446 (1961).

[20] E. Marshalek, L. Person and R.K. Sheline, Rev. Mod. Phys. 35, 108 (1963).

[21] D.A. Arseniev, A. Sobiczewski and V.G. Soloviev, Nucl. Phys. A139, 269 (1969).

[22] J. Meyer-ter-Vehn, Nucl. Phys. A249,111, 141 (1975).

[23] H. Toki and A. Faessler, Nucl. Phys. A253, 231 (1975) and Z. Physik A276, 35 (1976).

[24] F.S. Stephens, Rev. Mod. Phys. 47, 43 (1975).

[25] C. Ekström, S. Ingelman, M. Olsmats and B. Wannberg, Physica Scripta 6, 181 (1972).

[26] F.S. Stephens, R.M. Diamond, J.R. Leight, T. Kammuri and K. Nakai, Phys. Rev. Lett. 29, 438 (1972).

[27] R. Hayano et al., University of Tokyo, preprint, 1974.

[28] K. Wisshak, H. Klewe-Nebenius, D. Habs, H. Faust, G. Nowicki and H. Rebel, Nucl. Phys. A247, 59 (1975).

[29] H. Klewe-Nebenius, D. Habs, K. Wisshak, H. Faust, G. Nowicki, S. Göring, H. Revel, G. Schatz and M. Schwall, Nucl. Phys. A240, 137 (1975).

[30] D. Habs, G. Nowicki, H. Klewe-Nebenius, K. Wisshak, J. Buschmann, H, Tebel and G. Schatz, Proc. Int. Conf. on Nuclear Physics, Munich 1973, eds. J. de Boer and H.J. Mang (North-Holland, American Elsevier, 1973) p. 183.

[31] A.K. Gaigalas, T.E. Schroy, G. Schatz and D.B. Fossan, Phys. Rev. Lett. 35, 555 (1975).

[32] U. Hagemann and H.J. Keller, Proc. 3rd Int. Conf. on Nuclei far from Stability, Cargèse, 1976, CERN Report 76-13, p. 397.

[33] I. Rezanka, A. Kerek, A. Luukko and C.J. Herrlander, Nucl. Phys. A141, 130 (1970).

[34] J. Gizon, A. Gizon, M.R. Maier, R.M. Diamond and F.S. Stephens, Nucl. Phys. A222, 557 (1974).

[35] J. Gizon, A. Gizon and D.J. Horen, Nucl. Phys. A252, 509 (1975).

[36] J. Gizon, A. Gizon and J. Meyer-ter-Vehn, Nucl. Phys. A277, 464 (1977).

[37] G.P. Nowicki, J. Buschmann, A. Hanser, H. Rebel. H. Faust, D. Habs, H. Klewe-Nevenius and K. Wisshak, Nucl. Phys. A249, 76 (1975).

[38] J. Conrad, R. Repnow and J.P. Wurm, Proc. Int. Conf. on Reactions Between Complex Nuclei, Nashville, 1974, p. 153.

[39] D. Habs, H. Klewe-Nebenius, K. Wisshak, R. Löhken, G. Nowicki and H, Rebel, Z. Physik 267, 149 (1974).

[40] A. Bohr and B.R. Mottelson, K. Dan. Vidensk, Selsk. Mat.-Fys. Medd. 27, No 16 (1953).

[41] D.C. Choudhury, K. Dan. Vidensk. Selsk. Mat.-Fys. Medd. 28, No 4 (1954).

[42] I. Ragnarsson and S.G. Nilsson, Proc. of Colloquium on Intermedia.e Nuclei, Institut de Physique Nucléaire d'Orsay, 1971, p. 112.

[43] G. Beyer, R. Arlt, E. Herrmann, A. Jasinski, O. Knotek, G. Musiol, H.G. Ortlepp, H.V. Siebert and J. Tyrroff, Nucl. Phys. A260, 269 (1976).

[44] S. Ingelman, C. Ekström, M. Olsmats and B. Wannberg, Physica Scripta 7, 24 (1973).

[45] C. Ekström, S. Ingelman, M. Olsmats, B. Wannberg, G. Andersson and A. Rosén, Nucl. Phys. A196, 178 (1972).

[46] H. Fischer, private communication.

[47] C.J. Gallagher Jr and S.A. Moszkowski, Phys. Rev. 111, 1282, (1958).

[48] S. Ullrich and E.W. Otten, Nucl. Phys. A248, 173 (1975).

Table 1

Summary of results from the spin measurements in the cesium isotopes

Mass number A	Half-life $T_{1/2}$	Measured nuclear spin I
120	58 sec	2
121	2 min	$^3/_2$
121	2 min	$^9/_2$
122	21 sec	1
122m	4.2 min	8
123	5.8 min	$^1/_2$
124	30.8 sec	1
126	1.6 min	1
128	3.8 min	1
130m	3.7 min	5
135m	53 min	$^{19}/_2$

Table 2

Experimentally observed $\Delta F=1$ transitions in weak fields and $\Delta F=0$ transitions in strong external fields, together with results from the fitting procedure.

Isotope	Frequency of calibration transition in ^{39}K (MHz)	$\mu_B B/h$ (MHz)	Observed resonance frequency (MHz)	$g_I > 0$			$g_I < 0$		
				Residual (MHz)	χ^2	Hfs constant (MHz)	Residual (MHz)	χ^2	Hfs constant (MHz)
^{122}Cs	0.225(12)	0.449(24)	619.861 (3) [a]	0.000			0.000		
	0.225(12)	0.449(24)	620.454(15) [b]	-0.006			-0.006		
	36.531(17)	59.828(23)	45.378 (7)	-0.004			-0.009		
	108.470(30)	137.966(27)	122.482(15)	0.002			-0.007		
	200.110(40)	209.626(28)	210.990(20)	-0.003			-0.013		
	386.890(50)	326.432(29)	384.810(45)	-0.004	0.087	413.240(2)	-0.013	0.413	- 413.24(2)
^{123}Cs	108.488(18)	137.982(16)	140.260(15)	-0.001			-0.055		
	200.301(25)	209.760(17)	214.970(25)	0.001	0.004	8655 (45)	0.047	8.467	-9313 (52)
^{124}Cs	36.530(17)	59.826(23)	40.945 (7)	-0.001			-0.025		
	108.495(19)	137.988(17)	97.622(13)	0.003			-0.032		
	200.190(26)	209.682(18)	152.884(20)	-0.002			-0.028		
	386.927(30)	326.453(17)	249.900(25)	0.000	0.043	2099.0 (16)	0.032	7.671	-2109.5(16)
^{126}Cs	36.538 (7)	59.837(10)	40.810 (7)	-0.002			-0.028		
	108.485(18)	137.979(16)	96.842(10)	0.001			-0.034		
	200.313(30)	209.768(21)	151.125(20)	-0.009			-0.028		
	386.920(30)	326.449(17)	245.360(35)	0.007	0.201	2427.2 (26)	0.073	18.149	-2466.4(26)
^{128}Cs	36.540 (7)	59.840(10)	40.624 (8)	-0.004			-0.038		
	108.479(18)	137.974(16)	95.840(15)	-0.003			-0.053		
	200.150(29)	209.654(20)	148.710(20)	-0.002			-0.039		
	386.960(40)	326.472(23)	239.567(23)	0.004	0.221	3043.1 (35)	0.053	26.892	-3078.3(36)
^{130}Cs	200.270(40)	209.738(28)	145.735(22)	0.003			-0.071		
	386.975(40)	326.481(23)	232.057(21)	-0.001	0.008	4567.3 (79)	0.024	6.481	-4679.8(83)

a) $(^3/_2, ^1/_2) \leftrightarrow (^1/_2, -^1/_2)$, $(^3/_2, -^1/_2) \leftrightarrow (^1/_2, ^1/_2)$.

b) $(^3/_2, ^3/_2) \leftrightarrow (^1/_2, ^1/_2)$.

The remaining frequencies correspond to $\Delta F=0$ single-quantum transitions.

Table 3

Hyperfine structure (hfs) data and magnetic moments evaluated from the experimentally observed resonance frequencies

Mass number A	Nuclear spin I	Hfs separation $\Delta\nu$ MHz	Dipole constant a MHz	Magnetic moment μ_I n.m.*)
122	1	±619.860(3)	±413.240(2)	±0.133 (2)
124	1	3148.5 (24)	2099.0 (16)	0.674 (7)
126	1	3640.8 (39)	2427.2 (26)	0.779 (8)
128	1	4564.7 (53)	3043.1 (35)	0.977(10)
130	1	6851 (12)	4567.3 (79)	1.466(15)
123	½	8655 (45)	8655 (45)	1.389(16)

*) A hyperfine anomaly $^{A}\Delta^{133}$ = ±1% is assumed.

FIGURE CAPTIONS

Fig. 1 : Schematic drawing of the ABMR apparatus connected on-line with the ISOLDE isotope separator. (1)Beam line from the isotope separator, (2) off-line collector position, (3) vacuum chamber with electrostatic deflector plates, (4) beam line continuing to the optical pumping experiment, (5) beam scanner, (6) automatic valve, (7) electrostatic quadrupole triplet, (8) oven section of the ABMR apparatus, (9) sixpole focusing magnet, (10) dipole magnet and r.f. loop, (11) fourpole focusing magnet, (12) collector section, (13) collector disc supply , (14) on-line detector system. The lower part of the figure shows the beam space of the ABMR apparatus with a heavily enlarged radial scale. The beam bundle indicates atoms in resonance, i.e. those having undergone a transition from a focusing to a defocusing state. In off-resonance, the atoms hit the central obstacle in the analysing magnet.

Fig. 2 : Experimental yields of cesium isotopes from a 140 g/cm^2 lanthanum target irradiated by a 0.7 μA proton beam. Dots and squares indicate measurements using Faraday cup and beta counting, respectively. Our spin measurements are marked by crosses at the bottom of the figure, and previously known spins are marked by circles.

Fig. 3 : Neutralization efficiencies of the alkali elements potassium, rubidium and cesium as functions of surface work function. The temperature is assumed to be 1000^0 C.

Fig. 4 : Release of rubidium from an Y/Ta foil. The curves show the remaining activity in the foil relative to the initial activity as a function of heating time.

Fig. 5 : Delay time (in terms of the time for 50% release) as a function of the inverse of the absolute temperature. The corresponding temperatures in ^{0}C are indicated at the top. Note that the activation energy for diffusion of rubidium in yttrium is given by the slope of the line. The value of approximately 50 kcal/mol is typical for diffusion processes.

Fig. 6 : Energy level diagram of a spin I = 1 cesium isotope in the $^{2}S_{1/2}$ electronic ground state as a function of external magnetic field. A positive value of a is assumed. The single-quantum transition followed in the hyperfine structure measurements in $^{122,124,126,128,130}Cs$ is indicated by an arrow.

Fig. 7 a and b : Resonance curves of the single-quantum transition $(^{3}/_{2}, {}^{-1}/_{2}) \leftrightarrow (^{3}/_{2}, {}^{-3}/_{2})$ in ^{122}Cs and ^{130}Cs, respectively, recorded in an external magnetic field of 15.0 mT.

Fig. 8 : Block diagram of the r.f.-system used in the search for the $\Delta F = 1$ transitions in ^{122}Cs. A stable crystal-oscillator derived signal at 145.000 MHz is mixed in a doubly-balanced hot carrier diode ring mixer with the ≈ 10 MHz variable output from a programmable low-frequency synthesizer. The upper sideband component at 155 MHz is filtered out by a 5-pole bandpass filter, amplified 40 dB in a broadband amplifier and fed into a times-4 varactor multiplier. This yields an output power of about 2 W maximum into 50 Ω, at an efficiency of 25%, while suppressing the driving frequency and its other harmonics more than 26 dB referred to the output. The resolution of the output frequency is equal to the resolution of the low-frequency synthesizer times four, i.e. in this case

4 kHz. The primary source of drift was the 145 MHz source, which drifted about ± 2 ppm/h, but this could easily be corrected for by monitoring the 145 MHz signal with a frequency counter.

Fig. 9 : Results from the frequency scan for the $\Delta F = 1$ transitions in the isotope ^{122}Cs at an external field of about 30 μT. The FWHM of the "field independent" resonance line to the left is about 12 kHz.

Fig. 10 : Experimentally determined nuclear ground state magnetic moments of the cesium isotopes in the mass range 122-130. The moments of the odd-A isotopes, showing a small variation, are well accounted for by the predictions of the orbital $[420\ ^1/_2]$. In the doubly-odd isotopes, on the other hand, a drastic variation is evident (a negative value of the magnetic moment of ^{122}Cs is not excluded). The large difference between the moments of ^{122}Cs and ^{124}Cs may be explained by the configurations $1^+\{p[422\ ^3/_2]\ n[411\ ^1/_2]\}$ and $1^+\{p[420\ ^1/_2]\ n[411\ ^1/_2]\}$, respectively. We note, however, that both configurations violate the Gallagher- Moszkowski coupling rule of parallel intrinsic spins [47]. The moments of the heavier doubly-odd isotopes, being located in a transition region, are difficult to interprete in terms of simple configuration assignments. The shell-model configuration $1^+(pd_{5/2}\ nd_{3/2})$, with a magnetic moment of about 2 n.m. probably has an increasing influence as the shell closure at N = 82 is approached.

Fig. 11 : Portion of the nuclear chart showing stable and identified radioactive nuclides in the region $50 \leq (N,Z) \leq 82$. The cesium isotopes investigated in this work are indicated; nuclear spin measurements by a ring and hyperfine

structure by the symbol ◘ . The isodeformation curves for prolate deformations obtained in the Nilsson-model calculations of Arseniev et al.[20] are also shown. From these it is clear that the lightest cesium isotopes extend into regions with expected strong nuclear deformation. Ullrich and Otten [48] have made a systematic survey of deformation parameters from different experimental sources; isotope shifts, BE2-values and quadrupole moments, of iodine, xenon, cesium and barium isotopes in the corner $Z \geq 50$, $N \leq 82$. The theoretical deformation values shown in the figure are in qualitative agreement with the experimental data.

Fig. 12 : Nilsson diagrams for odd-proton and odd-neutron levels, calculated with the "extrapolated" shell parameters $\kappa_p = 0.0662$, $\mu_p = 0.540$ and $\kappa_n = 0.0637$, $\mu_n = 0.450$, and hexadecapole deformation parameter $\varepsilon_4 = 0$. Full lines represent levels with positive parity, dashed lines negative parity. The odd-proton levels $[420\ ^1/_2]$, $[422\ ^3/_2]$ and $[404\ ^9/_2]$, relevant to the discussion of the light cesium ($Z = 55$) isotopes, are drawn with heavy lines. Similarly, the odd-neutron level $[411\ ^1/_2]$, occupied by the 67th neutron for strong nuclear deformations, is emphasized.

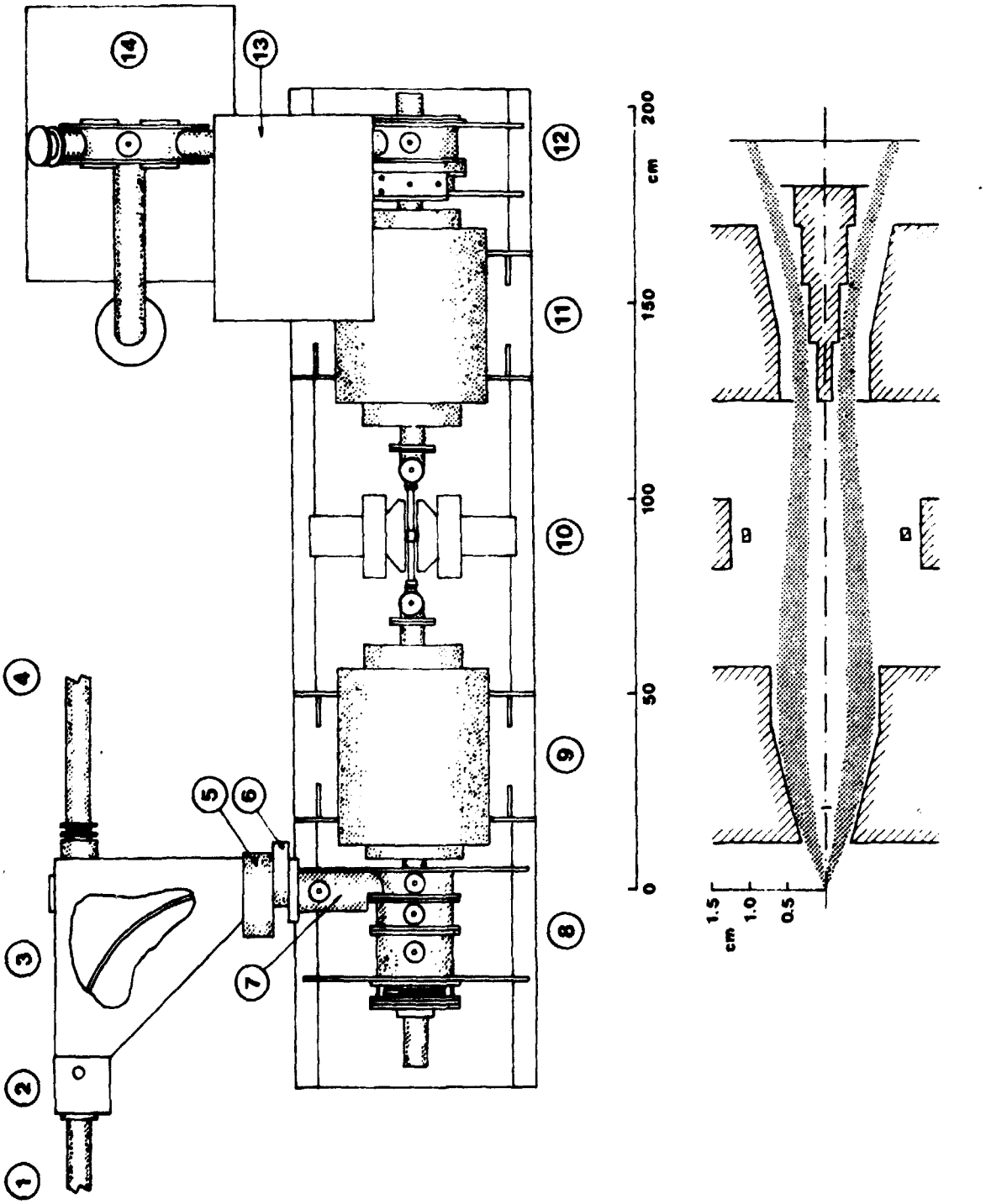

Fig. 1

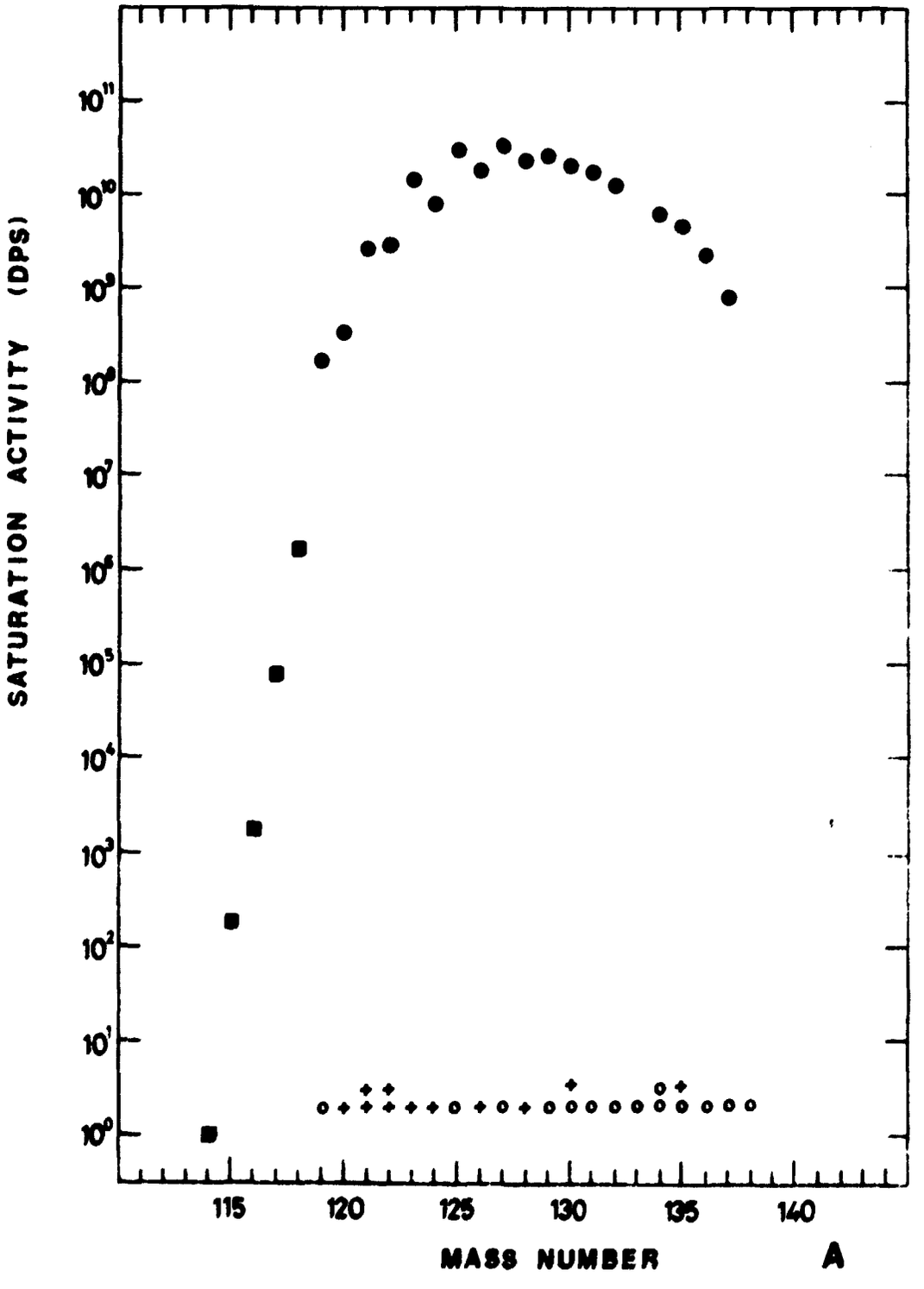
SATURATION ACTIVITY (DPS)
10^{11}
10^{10}
10^{9}
10^{8}
10^{7}
10^{6}
10^{5}
10^{4}
10^{3}
10^{2}
10^{1}
10^{0}
115
120
125
130
135
140
MASS NUMBER
A

Fig. 2

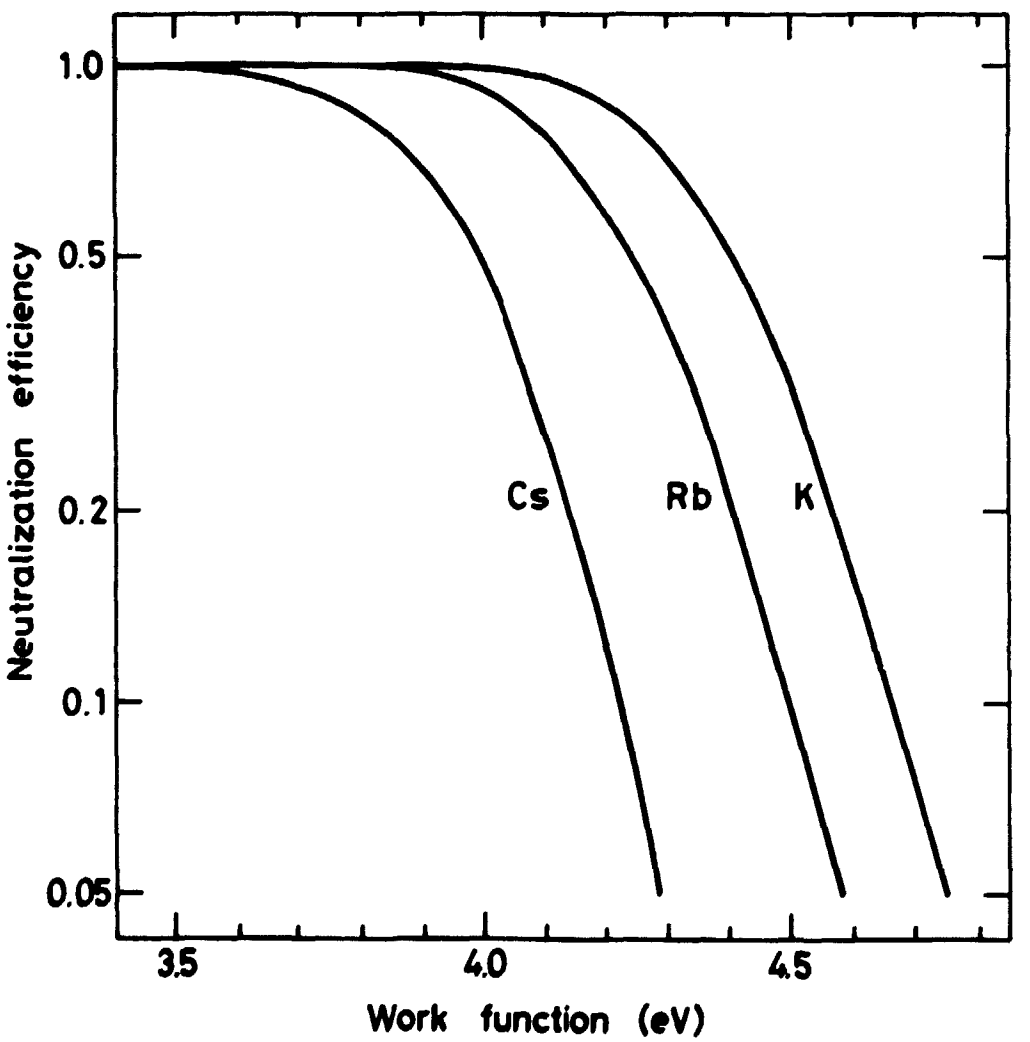
1.0
0.5
0.2
0.1
0.05
Neutralization efficiency
Cs
Rb
K
3.5
4.0
4.5
Work function (eV)

Fig. 3

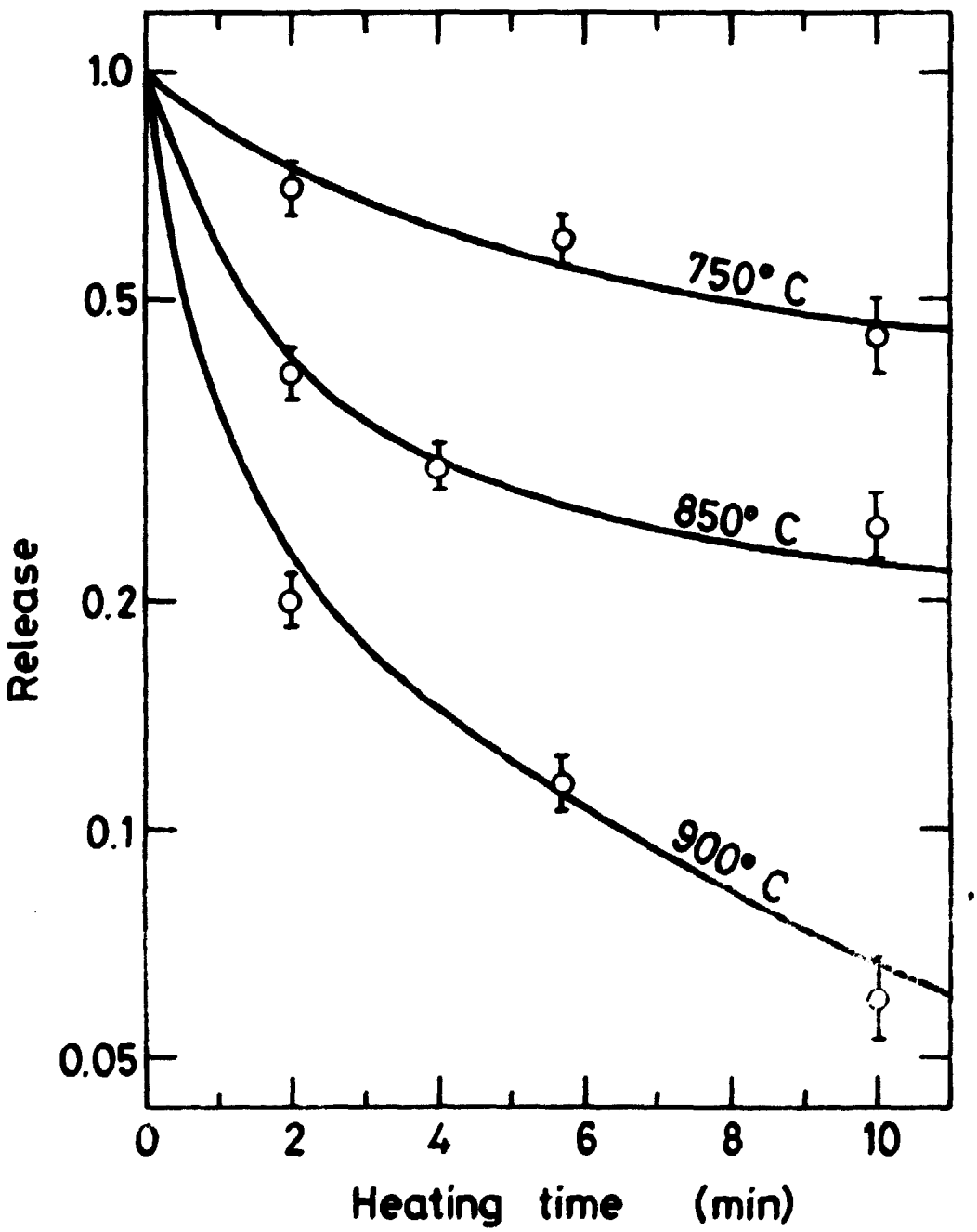
1.0
0.5
0.2
0.1
0.05
Release
750° C
850° C
900° C
0
2
4
6
8
10
Heating time (min)

Fig. 4

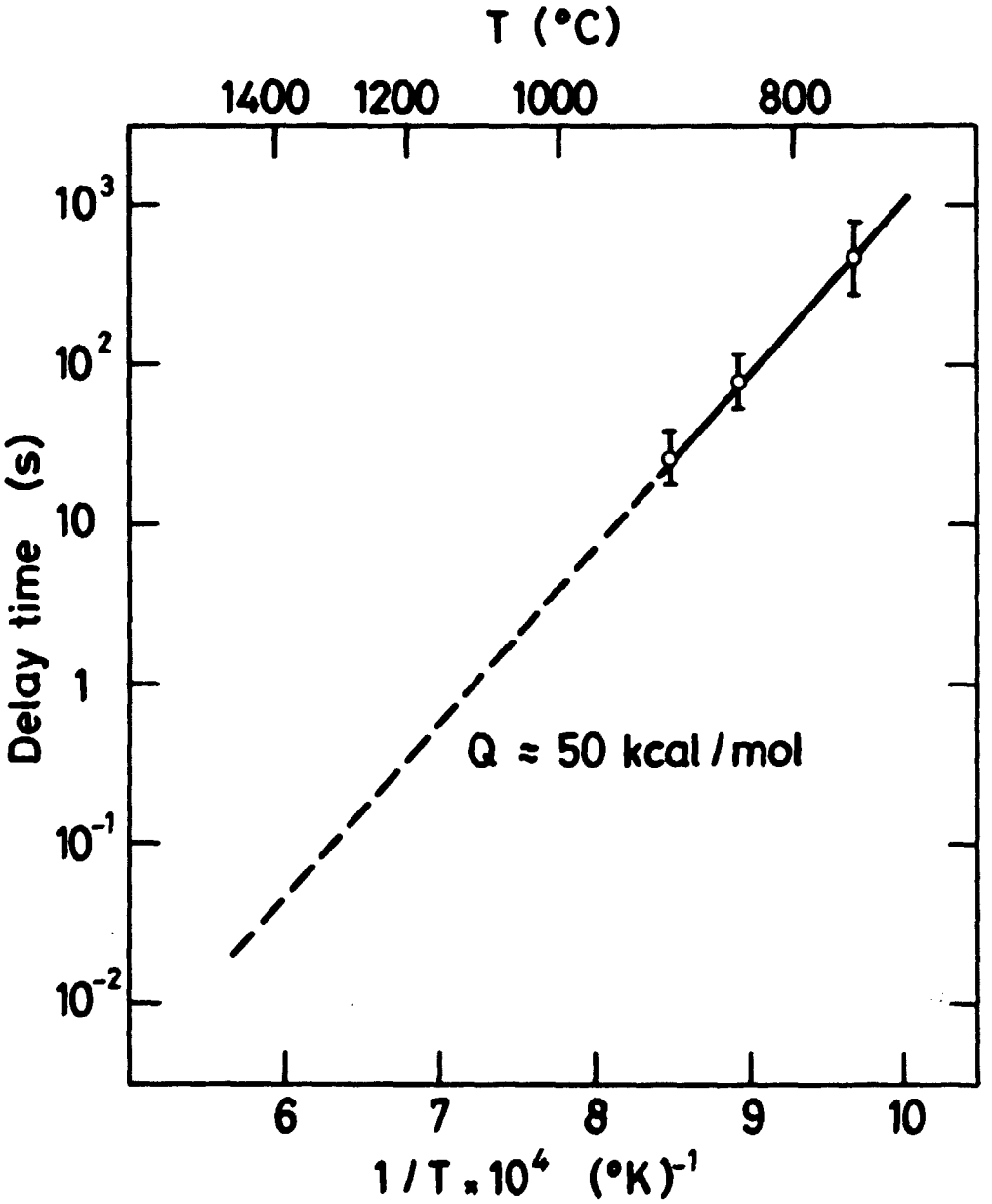
T (°C)
1400
1200
1000
800
10^3
10^2
10
1
10^{-1}
10^{-2}
Delay time (s)
Q ≈ 50 kcal / mol
6
7
8
9
10
1 / T . 10^4 (°K)$^{-1}$

Fig. 5

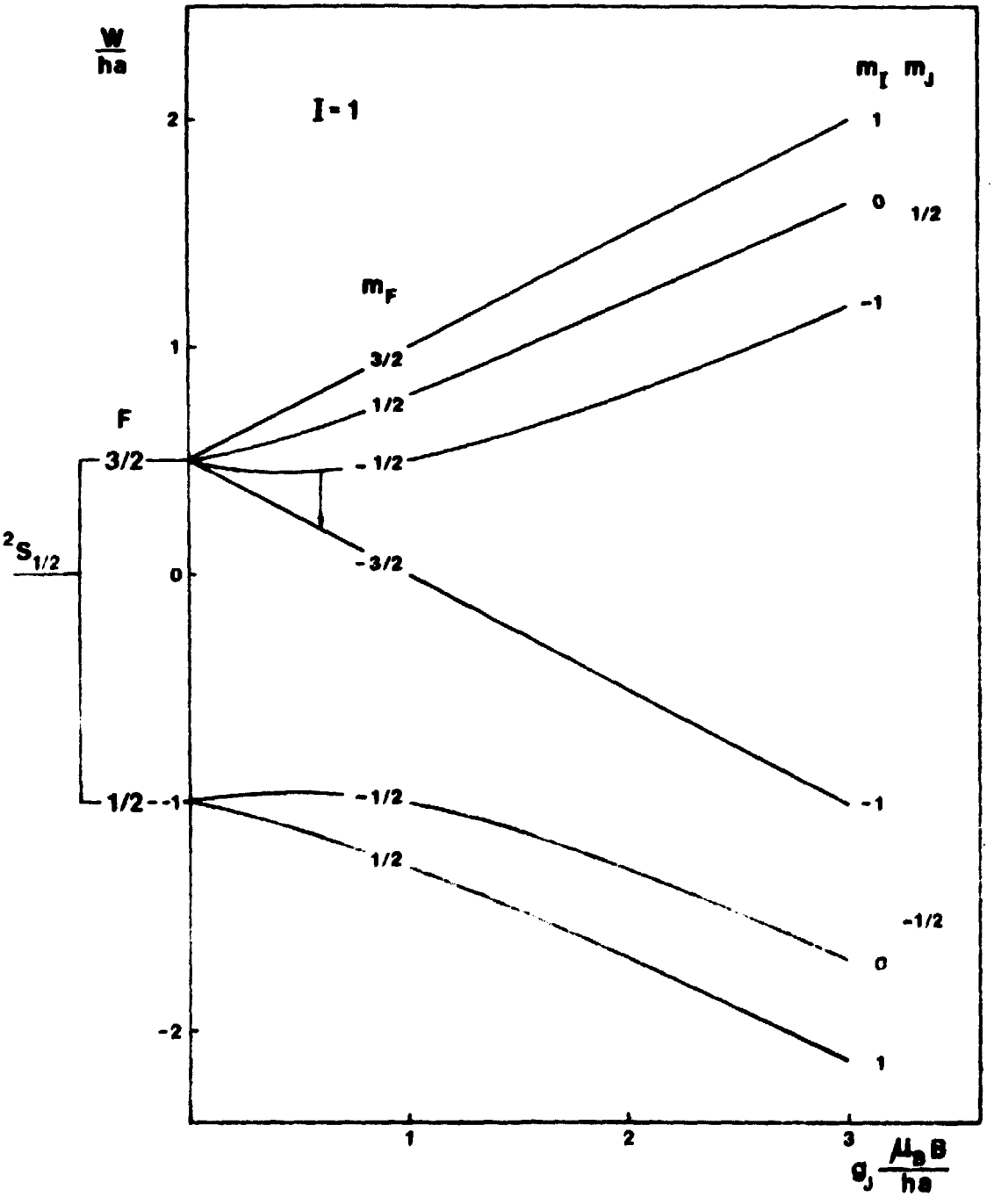
W/hA
I = 1
m_I m_J
2
1
0
-1
-2
m_F
3/2
1/2
-1/2
-3/2
F
3/2
1/2
$^2S_{1/2}$
1
0
-1
1/2
-1/2
-1/2
1/2
-1
1
0
1
2
3
$g_J \frac{\mu_B B}{hA}$

Fig. 6

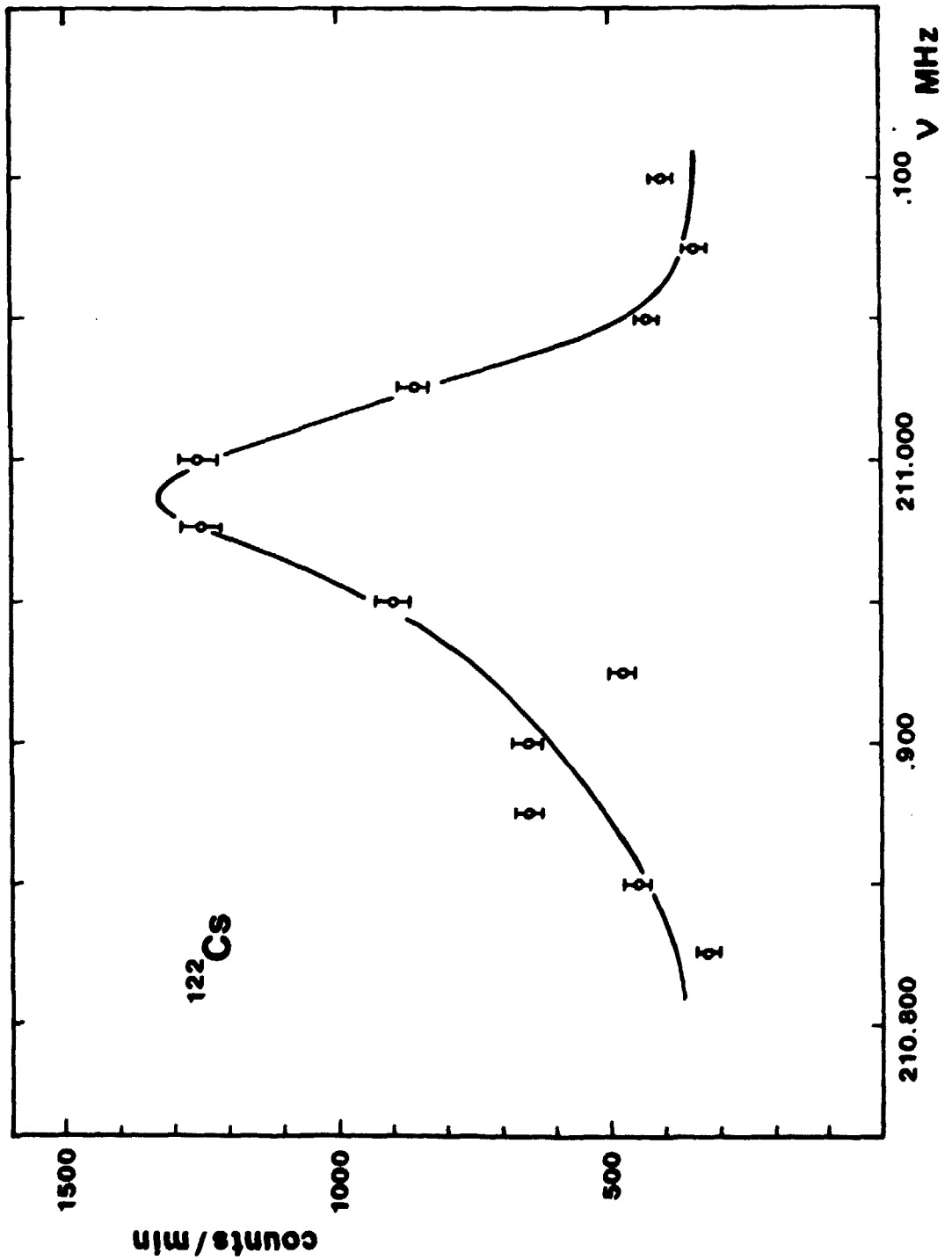

Fig. 7a

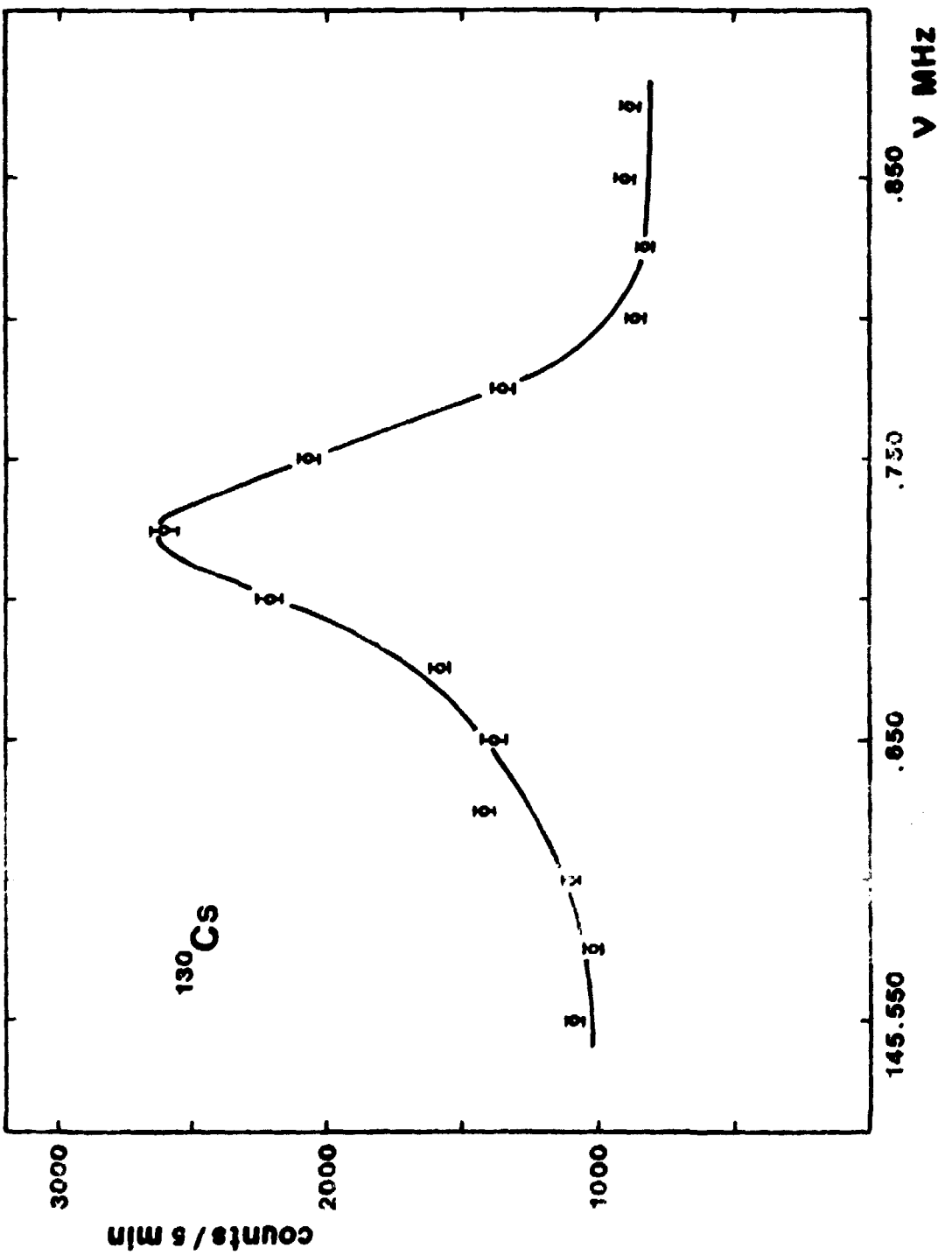

Fig. 7b

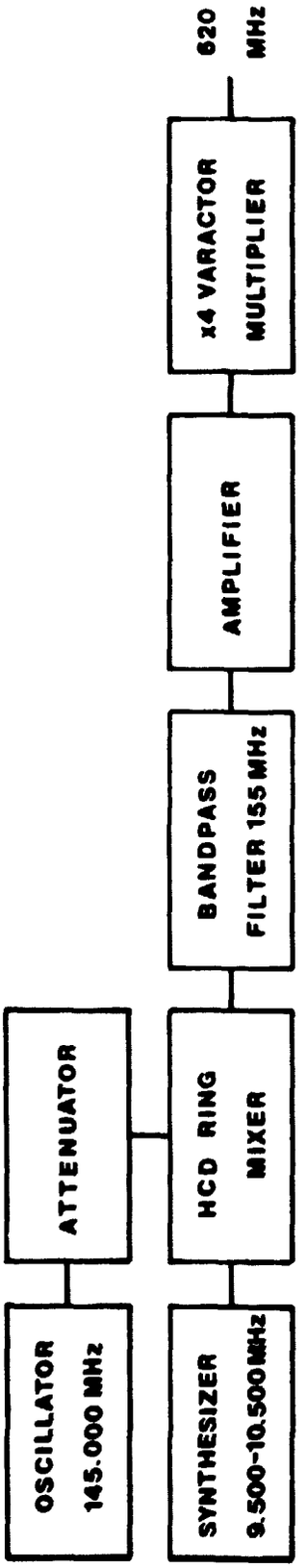
620 MHz
x4 VARACTOR MULTIPLIER
AMPLIFIER
BANDPASS FILTER 155 MHz
HCD RING MIXER
ATTENUATOR
OSCILLATOR 145.000 MHz
SYNTHESIZER 9.500-10.500 MHz

Fig. 8

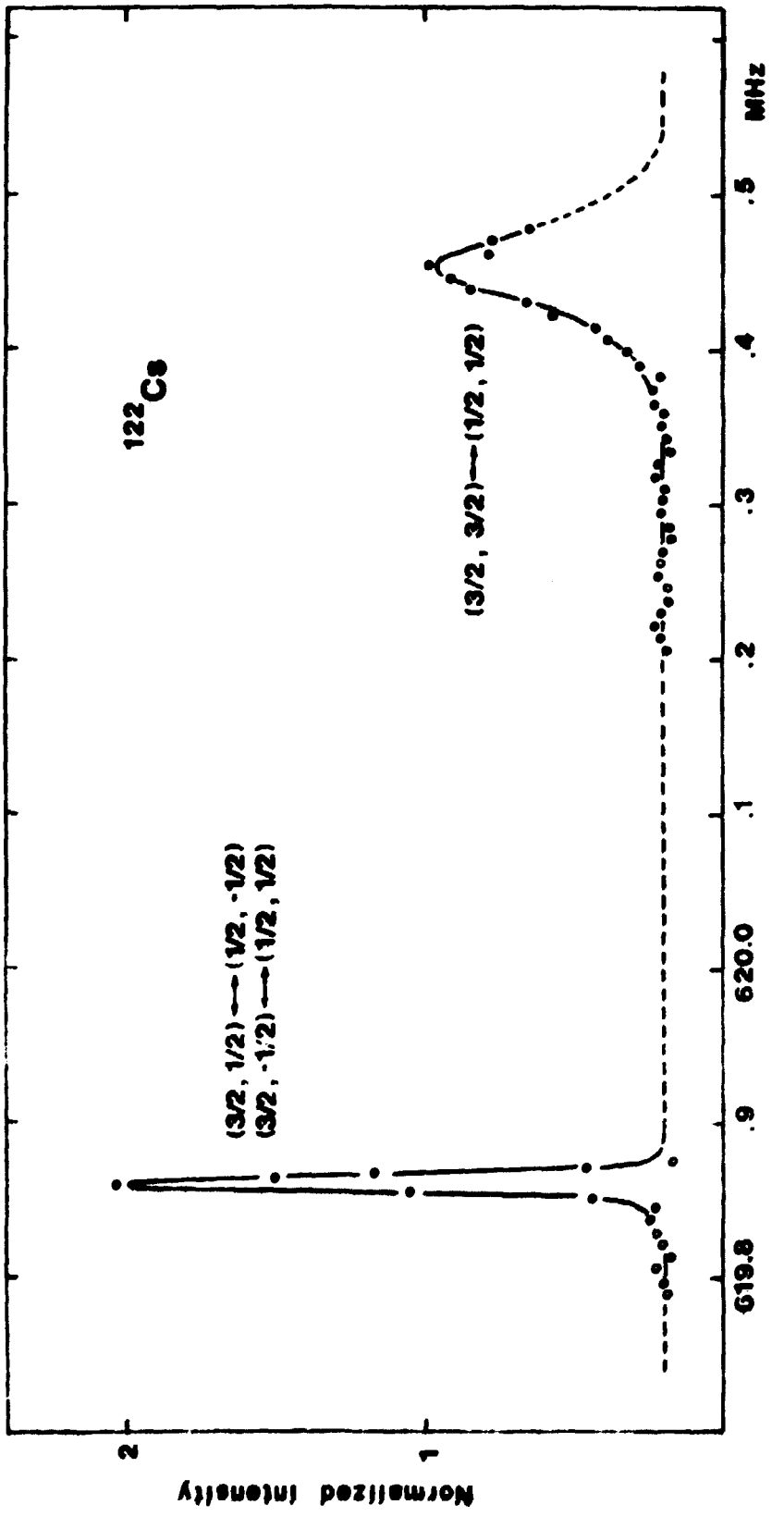
^{122}Cs
(3/2, 1/2) — (1/2, -1/2)
(3/2, -1/2) — (1/2, 1/2)
(3/2, 3/2) — (1/2, 1/2)
619.8
620.0
.9
.1
.2
.3
.4
.5
MHz
1
2
Normalized Intensity

Fig. 9

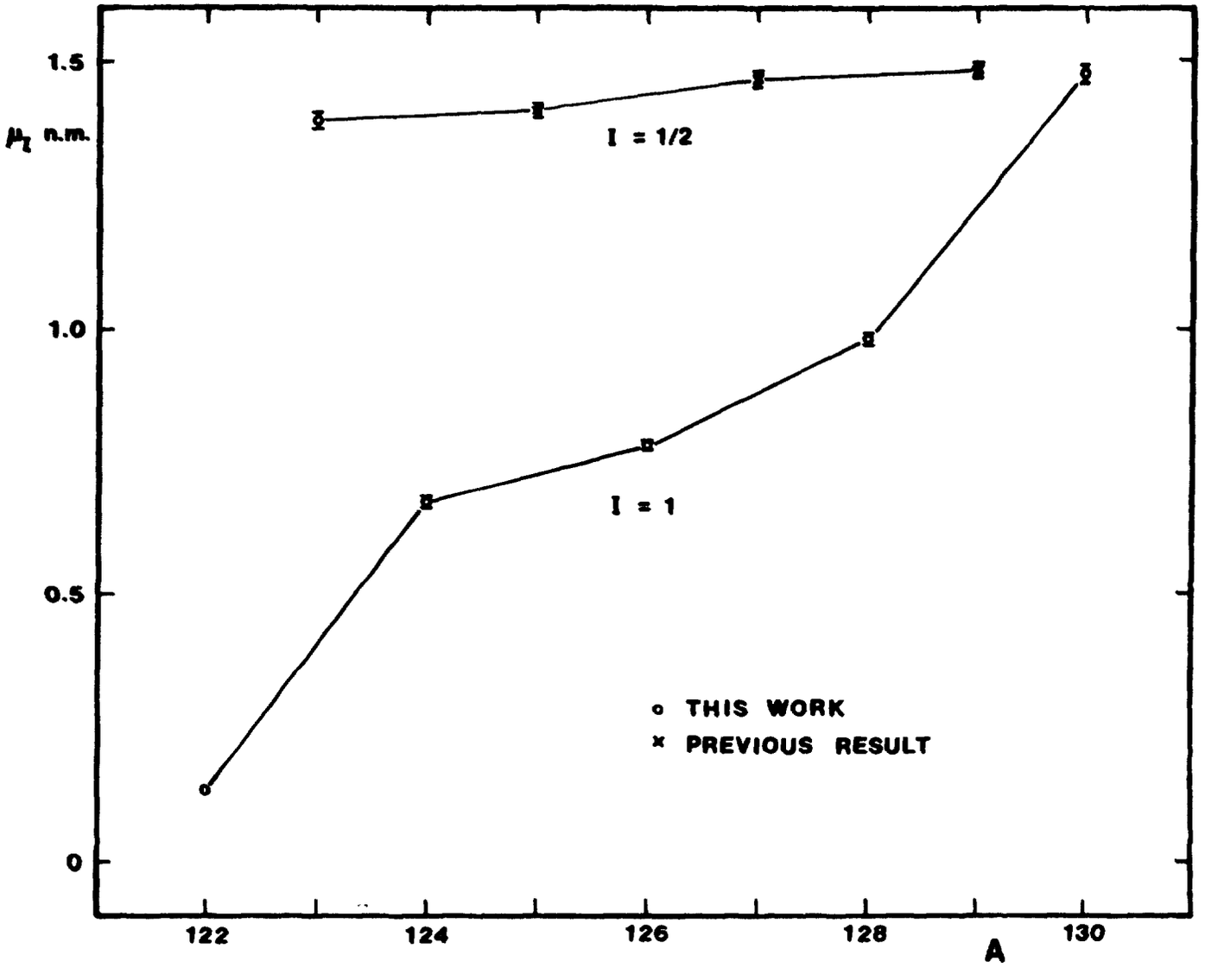
1.5
1.0
0.5
0
μ_I n.m.
I = 1/2
I = 1
o THIS WORK
× PREVIOUS RESULT
122
124
126
128
130
A

Fig. 10

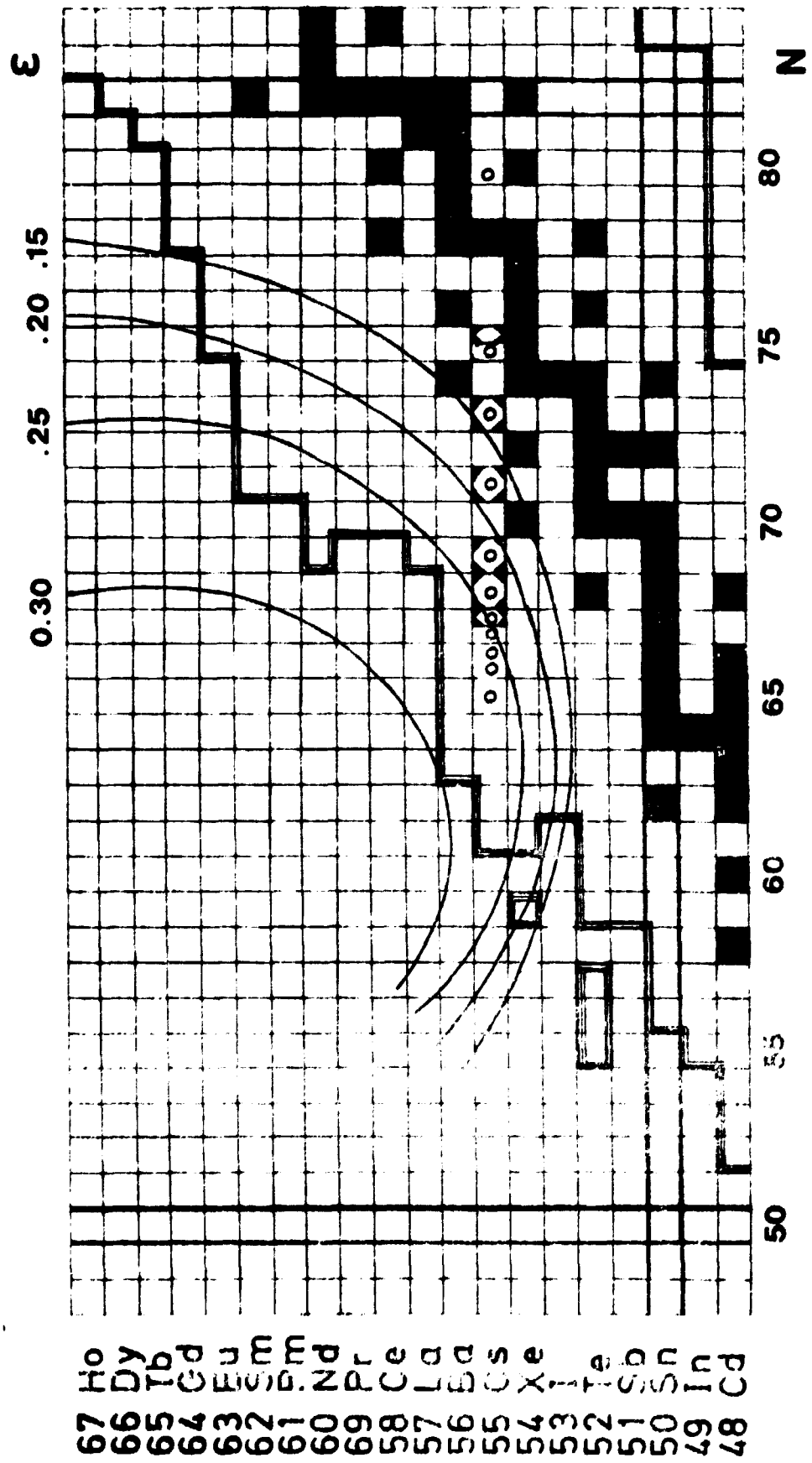
ε
N
0.30
.25
.20
.15
80
75
70
65
60
55
50
Ho Dy Tb Gd Eu Sm Nd Pr Ce La Ba Xe I Sn In Cd
67 66 65 64 63 62 61 60 59 58 57 56 55 54 53 52 51 50 49 48

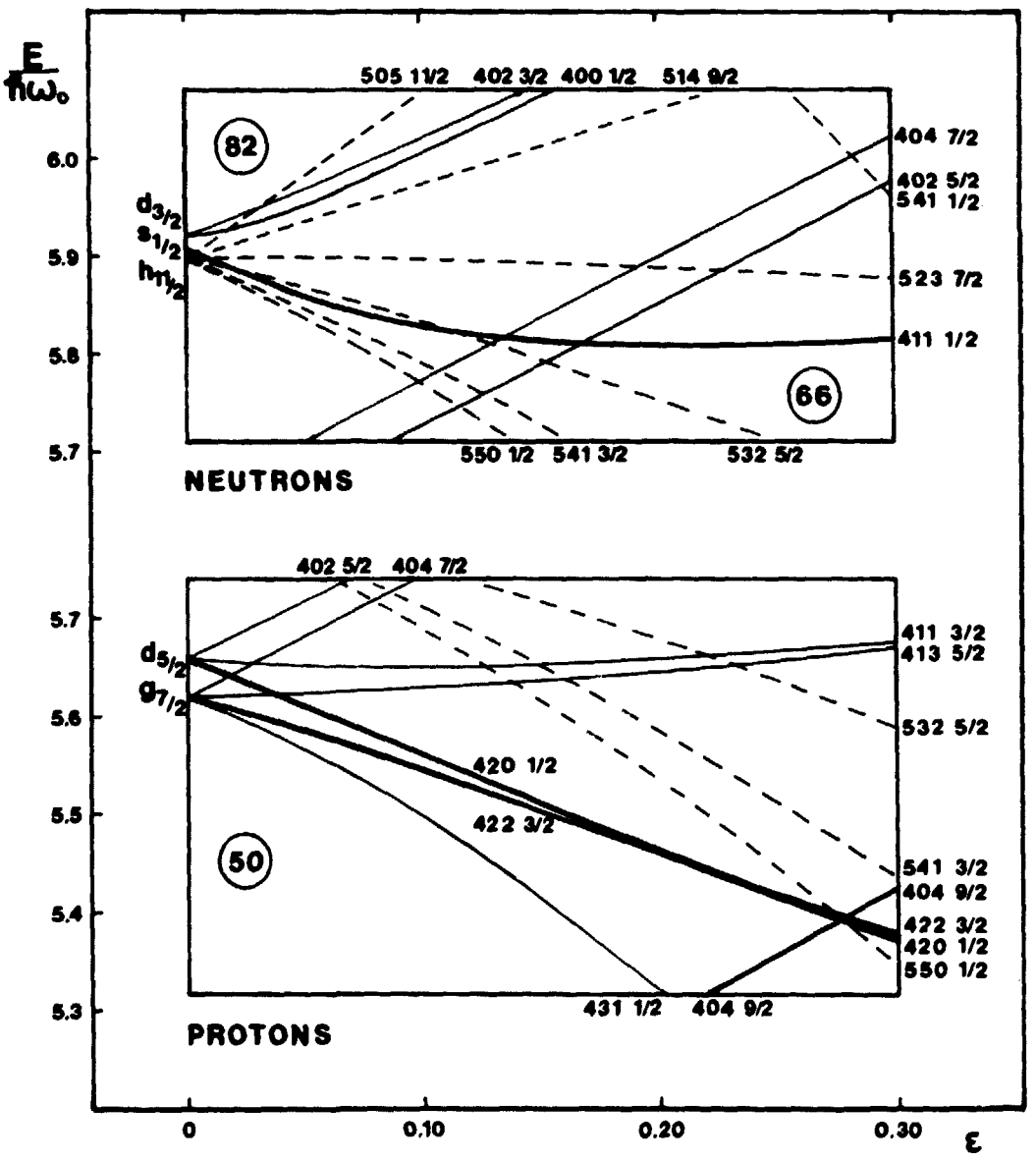
E/ħω₀
6.0
5.9
5.8
5.7
505 1/2
402 3/2
400 1/2
514 9/2
82
d3/2
s1/2
h11/2
404 7/2
402 5/2
541 1/2
523 7/2
411 1/2
66
550 1/2
541 3/2
532 5/2
NEUTRONS
5.7
5.6
5.5
5.4
5.3
402 5/2
404 7/2
d5/2
g7/2
411 3/2
413 5/2
532 5/2
420 1/2
422 3/2
50
541 3/2
404 9/2
422 3/2
420 1/2
550 1/2
431 1/2
404 9/2
PROTONS
0
0.10
0.20
0.30
ε

Fig. 12

ADDENDUM

to

HYPERFINE STRUCTURE, NUCLEAR SPINS AND MAGNETIC MOMENTS OF SOME CESIUM ISOTOPES

After the completion of the above paper we have measured the hyperfine structure in the isotopes ^{121}Cs and ^{130m}Cs at three external magnetic fields of strengths up to 5.5 mT. The reults are summarized below:

Nuclide	I	Hfs separation $\Delta\nu$ MHz	Dipole constant a MHz	Magnetic moment μ_I n.m. $^{+)}$
^{121}Cs	$^3/_2$	3220(18)	1610(9)	0.775(9)
^{130m}Cs	5	2151(14)	391.1(26)	0.628(8)

$^{+)}$ A hyperfine anomaly $A_\Delta{}^{133} = \pm$ 1 % is assumed.

The magnetic moment of ^{121}Cs, μ_I = 0.775(9), may be explained within the Nilsson model by assuming a nuclear deformation $\varepsilon \approx 0.25$. At this deformation the odd proton would occupy the orbital $[422\ ^3/_2]$, yielding μ_I = 0.8 n.m. ($g_s = 0.6 g_s^{free}$). The spin I = 5 of the isomeric state of ^{130}Cs has been interpreted as a $[420\ ^1/_2]$ proton orbital coupled to a $[514\ ^9/_2]$ neutron orbital, the latter originating in the $h_{11/2}$ shell model state. This configuration gives contributions to the magnetic moment of 1.5 n.m. and -0.7 n.m. for the odd proton and odd neutron, respectively.